Thermodynamics and pair structures of liquid alkali and alkaline-earth metals from the perturbative hypernetted-chain equation

Hong Seok Kang
Department of Chemistry and New Materials, College of Science and Engineering, Jeonju University, Hyoja-dong, Wansan-ku, Chonju, Chonbuk, Korea 560-759

(Received 25 November 1998; revised manuscript received 16 April 1999)

We have theoretically studied liquid alkali and alkaline-earth metals by combining the second-order pseudopotential (PP) theory of ion-electron interaction and a statistical mechanical method for calculating ionic thermal motion. The latter is done by utilizing the perturbative hypernetted-chain equation recently proposed by the author. The PP is modelled through an *ab initio* method presented by Shaw, i.e., through the use of the optimized nonlocal model potential (OMP). Calculations are carried out with two different methods for extracting parameters in the OMP. They are due to Animalu and Heine (AH), and Ballentine and Gupta (BG). Results show that both of thermodynamic properties and pair structures are in good agreements with experimental data for alkali metals with the AH set of parameters. For alkaline-earth metals other than Ba, calculations with the BG set give the radial distributions and structure factors in good agreement with experimental data. [S0163-1829(99)14533-8]

I. INTRODUCTION

Study of liquid metals are based on the combination of a quantum-mechanical theory of valence electrons and a statistical-mechanical method for ionic thermal motion. For alkali and alkaline-earth metals, the former problem is well solved by using the second-order pseudopotential theory for ion-electron interaction.[1] There are many different kinds of pseudopotentials in the literature. Adoption of a local model potential greatly simplifies the problem when the parameters in the potential are fitted to experimental data. We list only three of them: Ashcroft's empty-core pseudopotential (ECM),[2] Harrison's model potential,[1] and the most recent one due to Hasegawa.[3] These potentials were successfully applied to the study of the pair structures of liquid alkali metals with a judicious choice of the potential parameters.[4,5] However, it is well known that a consistent description of interaction of a valence electron with an ionic core requires a nonlocal and energy-dependent pseudopotential. For this, we recall that the ECM does not yield reliable pair structures of alkaline-earth metals.

The present work is concerned with optimized nonlocal model potential (OMP) proposed by Shaw[6–8] applied to the study of liquid metals. The OMP can be considered to be an *ab initio* pseudopotential in a sense that its parameters are obtained from atomic or ionic information, not from any information about a condensed phase. It was used by several authors to study simple metals and polyvalent metals.[9–11] However, attention was paid to either one of thermodynamic properties or pair structures. Reliable thermodynamics were obtained when the OMP was combined with Gibbs-Bogoliubov inequality or the perturbation theory of Weeks-Chandler-Anderson based on a reference system interacting with a simple model potential, not allowing quantitative description of pair structures.[12] Accurate description of the latter should be based on a more sophiscated theory such as the integral equation theory. For this purpose, Wax *et al.* recently showed that the soft mean-sphere approximation (SMSA) + OMP can be successfully applied to predict radial distribution functions $g(r)$ of alkali metals.[13] However, they found that Li was an exception in that the SMSA $g(r)$ is very different from either the experimental data or the computer-simulated data. This discrepancy was due to the inaccuracy of the SMSA for systems with a pair interaction whose hard-sphere packing fraction exceeds a certain value. For K and Rb, they also showed that the main peak of $g(r)$ is shifted toward smaller distances compared with experimental data. This is not only the case with the $g(r)$ calculated from the SMSA but also the case with that from the molecular dynamics simulation. Apparently, this reflects defect inherent in the OMP, noting that the shift can deteriorate predicted values of thermodynamic quantities too. In the next section, this problem will be reconsidered carefully, and it will be shown that a better estimation of input data for the OMP gives much more satisfactory results. This is not the only purpose of this work. Rather, we are more interested in the application of the perturbative hypernetted-chain (PHNC) equation to metallic systems.

Recently, the PHNC was successfully applied to model systems interacting with various kinds of model potentials.[14–16] Calculations showed that the accuracy of the theory is always comparable to the reference hypernetted-chain equation and Rosenfeld' density functional theory. The present work is concerned with its first application to metallic systems in combination with Shaw's OMP. Related to this, we consider other successful integral equation theories which can be applied to the metallic systems. These include the variational modified hypernetted-chain (VMHNC) integral equation[17,18] and the hybrid mean-spherical approximation (HMSA).[19] Researchers showed that the VMHNC can be widely used to predict static structure factors and thermodynamic properties of liquid metals. Various kinds of pseudopotentials were used together, including a nonlocal pseudopotential due to Li *et al.*[20] and local pseudopotentials

TABLE I. Parameters in the OMP used in this work at densities corresponding to Table II. Two different sets of data are shown for $A_0(E_f)$ and $A_1(E_f)$. The first line corresponds to the use of Animalu and Heine's method (AH) for the calculation of the core shift. The second line is due to Ballentine and Gupta's method (BG). See the text.

	Li	Na	K	Rb	Cs	Be	Mg	Ca	Ba
$A_0(E_f)$	0.331	0.309	0.241	0.228	0.207	1.014	0.782	0.576	0.461
	0.345	0.320	0.254	0.241	0.221	1.049	0.809	0.612	0.510
dA_0/dE	−0.183	−0.229	−0.312	−0.349	−0.389	−0.212	−0.289	−0.393	−0.475
$A_1(E_f)$		0.365	0.257	0.228	0.201		0.921	0.612	0.461
		0.367	0.261	0.232	0.207		0.924	0.620	0.477
dA_1/dE		−0.097	−0.166	−0.187	−0.214		−0.059	-0.141	−0.209

with parameters either from experiment[4,21] or from the *ab initio* calculation called neutral pseudoatom method (NPA).[22,23] Meanwhile, successful application of the HMSA appeared in the literature only in its combination with local model potentials.[24,25] This is related to the fact that there is difficulty in applying the HMSA to a metallic system, because of electronic inconsistency associated with the perturbative solution to the electronic energy.[26] In short, only the VMHNC has been shown to be generally applicable to the metallic systems. In this respect, it would be desirable to assess the reliability of the PHNC. In the next sections, this will be done for liquid alkali and alkaline-earth metals by comparing both of thermodynamic properties and pair structures with experimental data.

II. FORMULATIONS

In the OMP, the bare interaction $w_0(r)$ of a valence electron with an ionic core is considered to be described by Heine-Abarenkov potential[6–8]

$$w_0(r) = -\frac{Z_+ e^2}{r} - \sum_{l=0}^{l_0} \Theta[R_l(E) - r]\left[A_l(E) - \frac{Z_+ e^2}{r}\right] P_l, \tag{2.1}$$

where l_0 is the highest angular momentum quantum number for the core electrons, $R_l(E)$ and $A_l(E)$ are the radius and well depth of the core which depend on the energy eingenvalue of the system, P_l is the projection operator which extracts out the lth angular momentum component from the eigenfunction, $\Theta(r)$ is the heavyside step function, Z_+ is the valence charge of the ionic core. Shaw showed that the optimization of the model wave function is achieved by relating $A_l(E)$ and $R_l(E)$ by $A_l(E) = Z_+ e^2 / R_l(E)$.

$A_l(E)$ for a valence electron in the metal is calculated from the extrapolation of those for ionic term energies, assuming a linear dependence of $A_l(E)$ on the energy. Table I shows these parameters at the Fermi energy calculated from two different methods. Namely, core-shift of the electron energy due to the conduction electrons and all the ions other than that to which the electron belongs was calculated from the prescriptions given by Animalu and Heine (AH),[27,28] and Ballentine and Gupta (BG).[28,29] In the AH, the core shift $\Delta\epsilon_F$ at the Fermi level is approximated by an weighed average which places the most importance around $r \sim R_l$ by

$$\Delta\epsilon_F = -\mu_{xc} - \frac{Z_+ e^2}{2R_a}\left[3 - \frac{3}{4}\left(\frac{R_l}{R_a}\right)^2\right], \tag{2.2}$$

where μ_{xc} is the chemical potential due to the exchange and correlation effects for an electron gas of the number density Z_+/Ω, and R_a is the ionic radius. The BG uses a different weighing scheme which emphasizes small r more than large r by

$$\Delta\epsilon_F = -\mu_{xc} - \frac{Z_+ e^2}{2R_a}\left[3 - \frac{1}{6}\left(\frac{R_l}{R_a}\right)^2\right] \quad \text{if } l = 0,$$
$$= -\mu_{xc} - \frac{Z_+ e^2}{2R_a}\left[3 - \frac{1}{3}\left(\frac{R_l}{R_a}\right)^2\right] \quad \text{if } l > 0. \tag{2.3}$$

Here $R_l(E_F)$ and ϵ_F are obtained from the self-consistent iteration. For this, the values of $Z_+ R_l$ at experimental term energies are taken from Table 2 of Ref. 28. We find that the BG parameters shown in Table I are almost identical to those used by Wax *et al.*[13]

In the context of the second-order perturbation theory, the effective interaction $V(r)$ between a pair of ions is the sum of direct and indirect contributions. Namely,

$$V(r) = \frac{(Z_+^* e)^2}{r} + \frac{\Omega}{\pi^2}\int_0^\infty dq F(q)\frac{\sin(qr)}{qr} q^2, \tag{2.4}$$

where Z_+^* is the effective valence which takes into account the difference between the true wave function and the model pseudo-wave-function. Refer to Shaw's original paper for mathematical expression for this quantity. $F(q)$ is given by

$$F(q) = -\frac{2\Omega}{(2\pi)^3}\int_{k<k_F} \mathbf{dk}\frac{|w(\mathbf{k},\mathbf{q})|^2}{k^2 - |\mathbf{k}+\mathbf{q}|^2}$$
$$- \frac{2\pi e^2 \Omega}{q^2}\{G(q) n_d^2(q) + [1 - G(q)] n_{\mathrm{scr}}^2(q)\}, \tag{2.5}$$

where $w(\mathbf{k},\mathbf{q})$ is the atomic form factor between $\mathbf{k}$ and $\mathbf{k}+\mathbf{q}$ states, $n_d(q)$ and $n_{\mathrm{scr}}(q)$ are the Fourier transforms of the electron density due to the depletion hole and the first-order screening by other valence electrons, respectively. [Note that this equation is equivalent to Eq. (3.11) in Ref. 8.] We have assumed a uniform distribution of the depletion charge over an appropriate core volume. For the exchange-

TABLE II. Binding energy $E_{\rm bind}$ (in units of 10^{-3} a.u.) and the excess entropy S^e/k of liquid metals calculated from the present method in comparison with experimental data (Refs. 33,34). AH and BG denote that the corresponding quantities are calculated with the AH and the BG sets of the OMP parameters. See the text.

	T (K)	ρ (g/cc)	Ω (a.u.^{3})	$E_{\rm bind}$ Exp	$E_{\rm bind}$ AH	$E_{\rm bind}$ BG	S^e/k Exp	S^e/k AH	S^e/k BG
Na	378	0.928	277.61	−232.00	−235.02	−238.13	−3.45	−3.30	−3.08
K	343	0.826	530.42	−195.60	−200.07	−204.54	−3.45	−3.31	−2.93
Rb	313	1.476	648.88	−187.00	−192.29	−196.28	−3.63	−3.31	−2.87
Cs	303	1.838	810.29	−175.70	−180.76	−185.15	−3.56	−3.47	−2.94
Be	1521	1.690	59.76		−109.64	−110.75		−4.31	−4.05
Mg	953	1.545	176.28	−892	−903	−915	−3.41	−3.50	−3.24
Ca	1123	1.37	327.83	−732	−746	−764	−3.16	−3.82	−3.36
Ba	1003	3.32	463.52	−620[a]	−658	−682	−2.09(?)[a]	−4.94	−4.17

[a]Experimental data at 987 K quoted from Ref. 34.

correlation function $G(q)$, Ichimaru and Utsumi's (IU) expression is used throughout this work.[30]

Next, the PHNC equation for liquid can be described as below. First, the pair potential is divided into two parts. The reference potential $V_0(r)$ is chosen according to the prescription

$$V(r)=V_0(r)+V_1(r), \tag{2.6}$$

$$\begin{aligned} V_0(r)&=V(r)-F(r) \quad \text{if } r\leqslant\lambda, \\ &=0 \qquad\qquad\ \ \text{if } r>\lambda, \end{aligned} \tag{2.7}$$

$$\begin{aligned} V_1(r)&=F(r) \qquad\ \ \text{if } r\leqslant\lambda, \\ &=V(r) \qquad\ \ \text{if } r>\lambda. \end{aligned} \tag{2.8}$$

where $F(r)=V(\lambda)-V'(\lambda)(\lambda-r)$. In the case of model systems, two methods were suggested for determining λ. In a sophiscated version, it was chosen by requiring consistency of a thermodynamic function from two different routes. In this work, we adopt a simpler version, which can be expressed by

$$\lambda=\min(a_{fcc},r^*). \tag{2.9}$$

Here, $a_{fcc}=2^{1/6}/\rho^{1/3}$ is the nearest-neighbor distance for the face-centered-cubic lattice at a given density ρ; r^* is the distance at which the potential $V(r)$ attains its global minimum. In fact, we have smoothened this function so that λ is differentiable with respect to ρ at $\rho_0=\sqrt{2}/r^{*3}$. This is done by interpolating λ as a function of ρ within a narrow range around ρ_0, using a polynomial of degree 3. Its coefficients are obtained from the conditions that the function be continuous and have a continuous derivative with respect to ρ. In some cases, a metallic potential may possess more than one potential minimum at intermolecular seperations less than r^*. In the next section, it will be shown that this is the case of Be due to the strong Friedel oscillation. We are greatly interested in checking out if the PHNC needs any specific treatment in this case.

Once $V_0(r)$ is chosen, we approximate the bridge function $B(r)$ of the metallic system by that for the reference system. Namely,

$$B(r)\approx B_0(r), \tag{2.10}$$

and $B_0(r)$ is obtained from the Ballone *et al.* closure relation:[31]

$$B_0(r)=[1+s\,\gamma_0(r)]^{1/s}-1-\gamma_0(r), \tag{2.11}$$

where $\gamma_0(r)=g_0(r)-1-c_0(r)$, and $s=15/8$. [$c_0(r)$ is the direct correlation function.] This equation defines an approximate method to solve the Ornstein-Zernicke (OZ) relation for the reference system. A whole set of equations defined above give an approximate way of solving the OZ of the metallic system:

$$\gamma(r)\equiv h(r)-c(r)=\int d\mathbf{r}'c(r')h(|r-r'|), \tag{2.12}$$

where $h(r)=g(r)-1$ is the total correlation function. We have solved these equations numerically by using an efficient algorithm due to Gillan.[32]

Once the solution is found to the PHNC, the binding energy of the liquid metal is conveniently calculated from an expression in the Fourier space:

$$\begin{aligned} E_{\rm bind}(\Omega,T)=E_{\rm ind}(\Omega)&+\frac{\Omega}{2\pi^2}\int_0^\infty S(q)F(q)q^2dq \\ &+\frac{Z_+^{*2}e^2}{\pi}\int dq[S(q)-1]-E_{\rm IS}(Z_+^*), \end{aligned} \tag{2.13}$$

where the structure-independent energy $E_{\rm ind}(\Omega)$ is given by

$$E_{\rm ind}(\Omega)=E_{\rm vol}(\Omega)+E_{\rm IS}(Z_+^*), \tag{2.14}$$

with

$$E_{\rm vol}(\Omega)=Z_+(E_{\rm kin}+E_{xc})+\frac{9}{10}\frac{\rho_d^2e^2}{R_M}-\frac{3}{2}\frac{Z_+e^2\rho_d}{a_{WS}}+\frac{1}{N}\sum_{k<k_F}\langle k|w^R|k\rangle+\sum_{k<k_F}\sum_{l<l_0}\frac{dA_l}{dE}\langle k|P_l|k\rangle[\langle k_F|w^R|k_F\rangle-\langle k|w^R|k\rangle]. \quad (2.15)$$

Here, $S(q)=1+\rho h(q)$ is the static structure factor of the liquid metal. The second term in Eq. (2.13) is band-structure energy, and the remaining two terms comprise a structure-dependent contribution $E_{\rm str}^{es}$ to the electrostatic energy of positive charges Z_+^*e embedded in a uniform compensating background, where $E_{\rm IS}(Z_+^*)[=-0.9(Z_+^{*2}e^2/a_{\rm WS})]$ is the ion-sphere energy, i.e., the electrostatic energy of a positive charge Z_+^*e in a uniform neutralizing sphere of the radius equal to the Wigner-Seitz radius $a_{\rm WS}$. $E_{\rm vol}(\Omega)$ is the term depending only upon the density of the system. Four terms in its expression represent (1) the energy of the electron liquid, (2) interaction between depletion holes (ρ_d and R_M represent the depletion charge and the radius of the sphere in which the charge is distributed), (3) the interaction of an electron uniformly distributed over the Wigner-Seitz cell with the depletion hole, and (4) the non-Coulombic contribution of the bare model potential w^R given by the second term in Eq. (2.1).

The Helmoltz free energy $A(\Omega,T)$ is calculated from the relation

$$A(\Omega,T)=E_{\rm bind}(\Omega,T)+E_{\rm gas}-T[S^e+S_{\rm gas}], \quad (2.16)$$

where $E_{\rm gas}$ and $S_{\rm gas}$ are the energy and the entropy of the ideal gas. The excess entropy S^e is equivalent to that for a system interacting with a pair potential given in Eq. (2.4), not including the volume-dependent term. In order to calculate this quantity, we need the excess internal energy U^e and the excess Helmholtz free energy A^e for that system. The former quantity is calculated from the relation

$$\beta U^e=\frac{\beta\rho}{2}\int \mathbf{dr}V(r)g(r), \quad (2.17)$$

where $\beta=1/kT$. In order to calculate A^e, we first calculate the free energy (A_0^e) for a system interacting with $V_0(r)$ given in Eq. (2.7). This is done by integrating the compressibility factor $Z=P/\rho kT$ of the system as a function of density:

$$\beta A_0^e=\int_0^\rho\frac{[Z(\rho')-1]}{\rho'}d\rho'. \quad (2.18)$$

Following the spirit of the PHNC, values of $Z(\rho')$ at various densities $\rho'(<\rho)$ are again calculated from the solution of the OZ relation using Ballone *et al.*'s closure relation. Finally, A^e is obtained from the formulation in Ref. 17. To be more specific, the calculation is based on Eqs. (10)–(15) of Ref. 17 using A_0^e from Eq. (2.18).

TABLE III. Compressibility factor Z of liquid metals calculated from the numerical differentiation of the Helmholtz free energy with respect to density. Thermodynamic states considered in the calculation are given in Table I. The first and the second lines for each metal correspond to the AH and the BG sets of the OMP parameters. $Z_{\rm ind}^{\rm loc}$ and $Z_{\rm ind}^{\rm nl}$ correspond to contributions from the local and nonlocal terms in the structure-independent energy given in Eqs. (2.14) and (3.1); $Z_{\rm str}$ is the structure-dependent contribution from the terms other than $E_{\rm ind}(\Omega)$ in Eq. (2.13); Z_s is the entropic contribution.

	$Z_{\rm ind}^{\rm loc}$	$Z_{\rm ind}^{\rm nl}$	$Z_{\rm str}$	Z_s	Z
Na	−9.26	0.97	−2.23	4.40	−6.11
	−13.74	0.04	0.04	4.61	−9.05
K	−7.74	−3.49	−2.58	5.01	−8.80
	−14.80	−3.97	1.02	5.29	−12.47
Rb	−7.29	−6.94	−1.88	5.35	−10.76
	−15.73	−6.62	2.29	4.44	−15.62
Cs	−3.81	−10.14	−1.29	4.97	−10.26
	−14.57	−8.86	1.60	5.15	−16.68
Be	−3.00	16.30	−16.87	4.84	1.28
	−7.23	13.51	−11.97	4.45	−1.24
Mg	−16.50	2.83	3.77	6.31	−3.58
	−21.62	0.88	7.10	4.72	−8.92
Ca	−4.22	−2.88	−1.53	5.36	−3.27
	−12.17	−5.02	2.62	4.54	−10.03
Ba	13.67	−11.95	−18.20	5.16	−11.32
	−3.67	−13.47	−4.31	4.72	−16.73

III. RESULTS

Table II shows the binding energy $E_{\rm bind}$ and reduced excess entropy S^e/k of alkali and alkaline-earth metals calculated from the OMP+PHNC in comparison with experimental data. Thermodynamic states considered in the table correspond to those near freezing transition. As mentioned in the previous section, our calculation is based on two different treatments for the core shift, and we find that our results are sensitive to its choice. For alkali metals, predictions of the PHNC for both of $E_{\rm bind}$ and S^e/k are in good agreement with experimental data, when the AH set of parameters are used in the OMP. The BG set gives much less reliable results for all the quantities investigated. This behavior becomes less pronounced for the alkaline-earth metals, the BG set exhibiting the reliability comparable to that for the AH. Table III gives comparisons of the compressibility factor calculated from the numerical differentiation of the Helmholtz free energy. The table shows that $Z_{\rm ind}^{\rm nl}(=Z_{\rm ind}-Z_{\rm ind}^{\rm loc})$, the nonlocal contribution of $E_{\rm ind}(\Omega)$ to the compressibility factor Z, is comparable to its local correspondent $Z_{\rm ind}^{\rm loc}$, in its magnitude. For this, we define $E_{\rm ind}^{\rm loc}(\Omega)$ by

$$E_{\rm ind}^{\rm loc}(\Omega)=Z_+(E_{\rm kin}+E_{xc}+\langle\overline{k|w^R|k}\rangle)+E_{\rm IS}(Z_+e), \quad (3.1)$$

where $E_{\rm kin}$ and E_{xc} represent the kinetic energy and the exchange-correlation energy, repectively. $\langle\overline{k|w^R|k}\rangle$, which is the average of w^R, is defined by a relation similar to that in Eq. (2.11) of Ref. 35. Note that the ion-sphere energy is for the valence charge Z_+e, not for Z_+^*e. Equation (2.14) shows

TABLE IV. The long wavevector limit $S(k\rightarrow 0)$ of the static structure factor for liquid metals calculated from the OMP+PHNC in comparison with experimental data (Ref. 36) at thermodynamic states considered in Table I. The present calculation is based on two different sets of the OMP parameters, which are denoted by AH and BG. See the text.

	Na	K	RB	Cs	Be	Mg	Ca	Ba
Exp	0.023	0.023	0.022	0.024		0.025	0.031	0.035
AH	0.031	0.031	0.031	0.025	0.015	0.028	0.021	0.010
BG	0.040	0.050	0.052	0.045	0.016	0.030	0.026	0.014

that $Z_{\rm ind}^{\rm nl}$ is directly related to the core structure, in that it includes contributions from the depletion hole and the non-Coulombic interaction w^R in the bare model potential. In many cases, $Z_{\rm ind}^{\rm nl}$ is negative and its absolute value is large, when the total compressibility is also negative and has a large absolute value. Presumably, this implies that the negative values of the pressure are partly associated with a crude description of the core structure through the approximation of the uniform distribution of the depletion hole in an appropriate volume. Table IV gives a comparison of the long wavelength limit of the static structure factor $S(k\rightarrow 0)$ calculated from the present method with experimental data. It is worth mentioning that the AH generally gives $S(k\rightarrow 0)$ in better agreements with experimental data for alkali metals. Theoretical predictions are especially poor for Ba, and it can be ascribed to the partial filling of d states as will be described later in this section.

Next, we consider the pair structures of alkali metals calculated from the OMP+PHNC. Figures 1 and 2 show $S(k)$ and $g(r)$ for liquid potassium at the thermodynamic state considerd in Table II in comparison with experimental data. Similar plots are given for liquid rubidium in Figs. 3 and 4. In Fig. 1, two sets of experimental data are shown. This is to show uncertainties in the experimental data. One is due to Waseda at 70 °C,[37] and the other is due to Huijben and van der Lugt at 65 °C.[38] Experimental data in Figs. 2–4 correspond to Waseda's results. In all these figures two sets of theoretical data are shown, which are again based on the AH

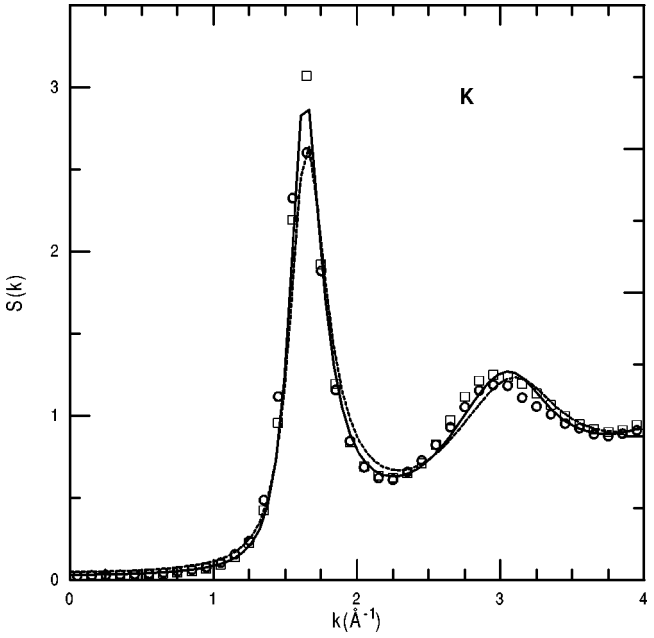

FIG. 1. $S(k)$ of liquid K at $T=343$ K and $\rho=0.826g/cc$. Two sets of experimental data are shown: open circles denote Waseda's data at 343 K (Ref. 37), and the open squares are due to Huijben and van der Lugt at 338 K (Ref. 38). Also shown are theoretical results from the OMP+PHNC. The solid line represents the use of the AH set of the OMP parameters, and the dashed line corresponds to the BG set.

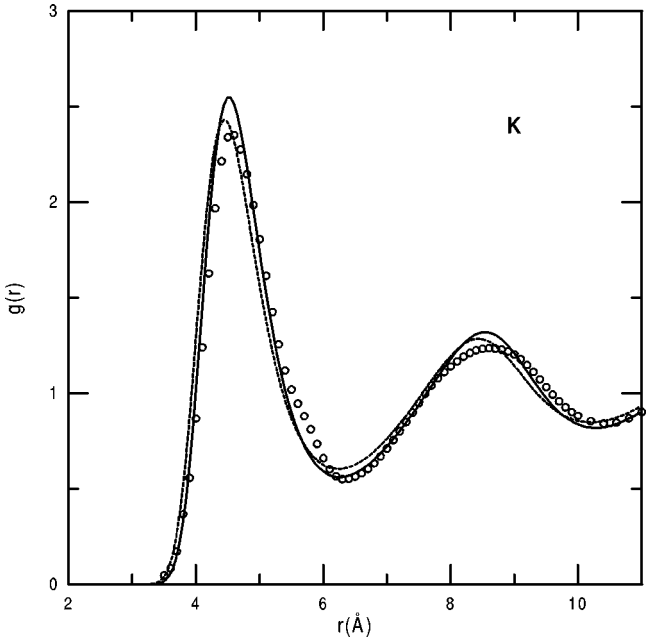

FIG. 2. $g(r)$ for liquid K at $T=343$ K and $\rho=0.826g/cc$. Open circles denote Waseda's experimental data (Ref. 37). Solid and dashed lines correspond to theoretical results from the OMP +PHNC calculated with the AH and the BG sets of the OMP parameters, respectively.

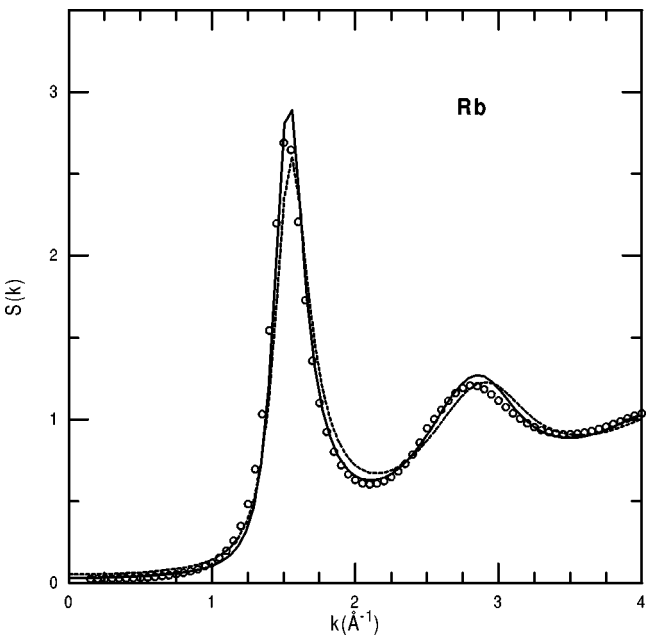

FIG. 3. $S(k)$ of liquid Rb at $T=313$ K and $\rho=1.476g/cc$. Notations are the same as in Fig. 2.

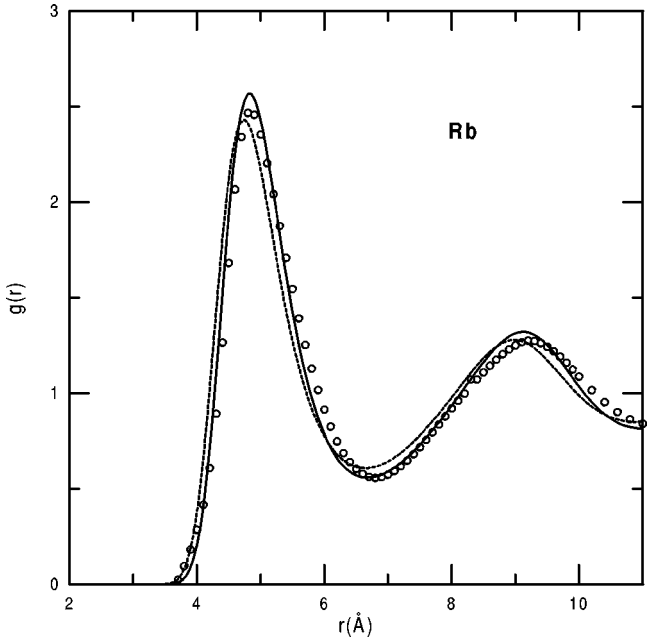

FIG. 4. $g(r)$ of liquid Rb at $T=313$ K and $\rho=1.476g/cc$. Notations are the same as in Fig. 2.

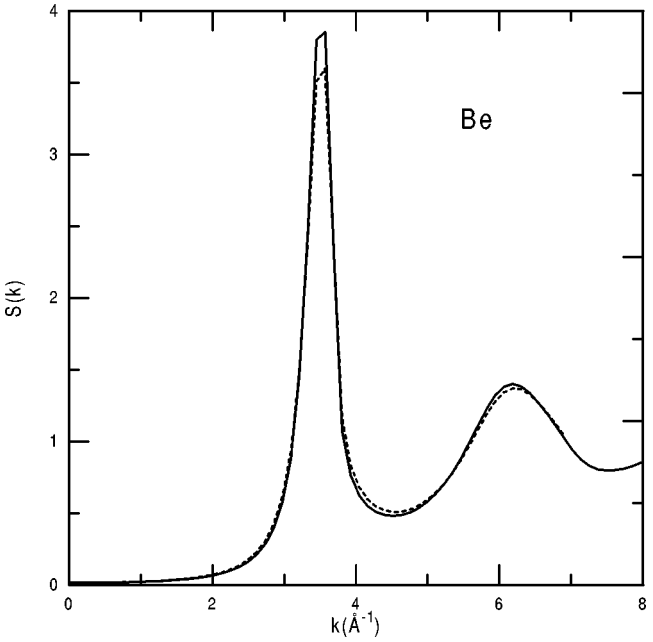

FIG. 6. $S(k)$ of liquid Be at $T=1521$ K and $\rho=0.11293A^{-3}$. Notations are the same as in Fig. 2.

(solid lines) and the BG parameters (dashed lines) for the OMP. In Fig. 1, we find that there is a large difference in the first peak of $S(k)$ between the two sets of experimental data, even if we take into account the fact that temperatures are different by 5 °C. As pointed out by Gonzalez *et al.*[23] comparison with other experimental data shows that the first peak in Waseda's data are systematically lower by an average of 10%. This will also introduce uncertainties in his $g(r)$, since it is obtained from the Fourier transform of $S(k)$. Therefore, we can conclude that $S(k)$ and $g(r)$ calculated from the OMP+PHNC are in good agreements with experimental data for alkali metals, when the AH parameters are used in the OMP. We also note that the BG $g(r)$'s calculated from the PHNC are almost identical to the Wax *et al.* result obtained from the molecular dynamics calculation based on the OMP with the same BG parameters. In particular, heights of the first two maxima in the PHNC $g(r)$ are approximately the same as in the simulated data. This can be easily seen from the comparsion of Figs. 2 and 4 with Fig. 3 of Ref. 13. This gives an indirect support for the reliability of the PHNC. Furthermore, this implies that the observed deviations of theoretical data from the experimental results are not

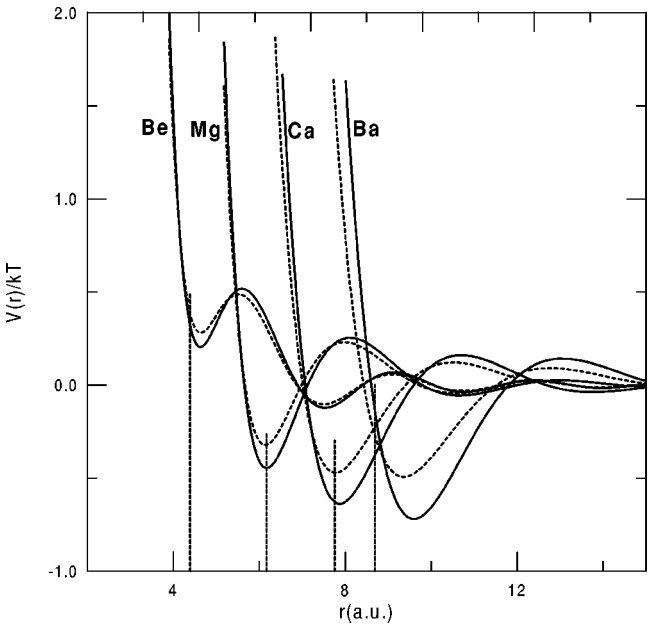

FIG. 5. Pair potential $V(r)$ of four liquid alkaline-earth metals at thermodynamic conditions shown in Table II. Solid and dashed lines represent the OMP+PHNC results with the AH and the BG sets of the OMP parameters, respectively. Vertical lines correspond to the breakpoint λ of the pair potential in the PHNC.

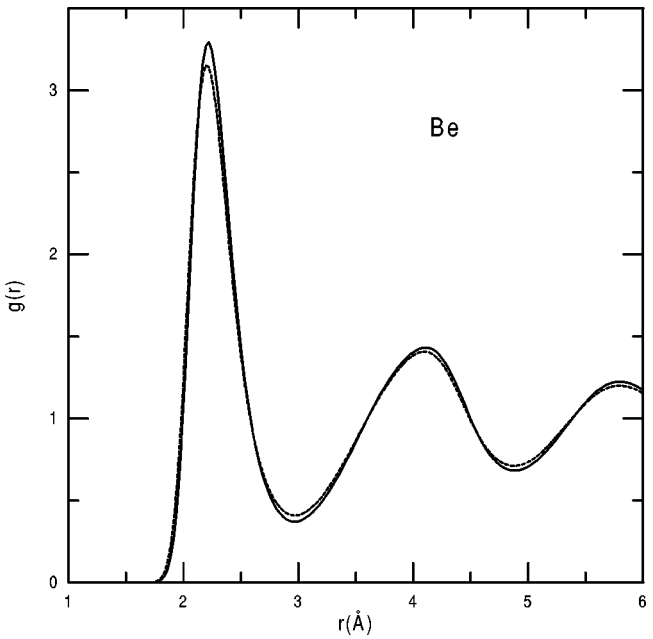

FIG. 7. $g(r)$ of liquid Be at $T=1521$ K and $\rho=0.11293A^{-3}$. Notations are the same as in Fig. 2.

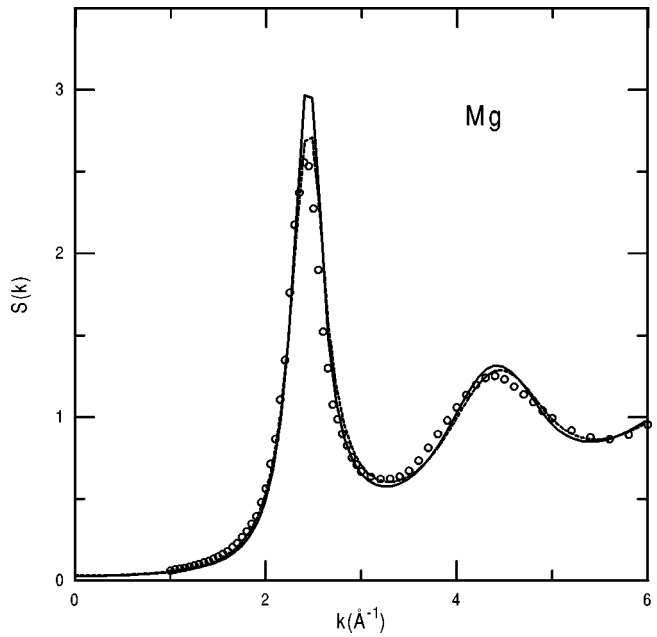

FIG. 8. $S(k)$ of liquid Mg at $T=953$ K and $\rho=0.03829A^{-3}$. Notations are the same as in Fig. 2.

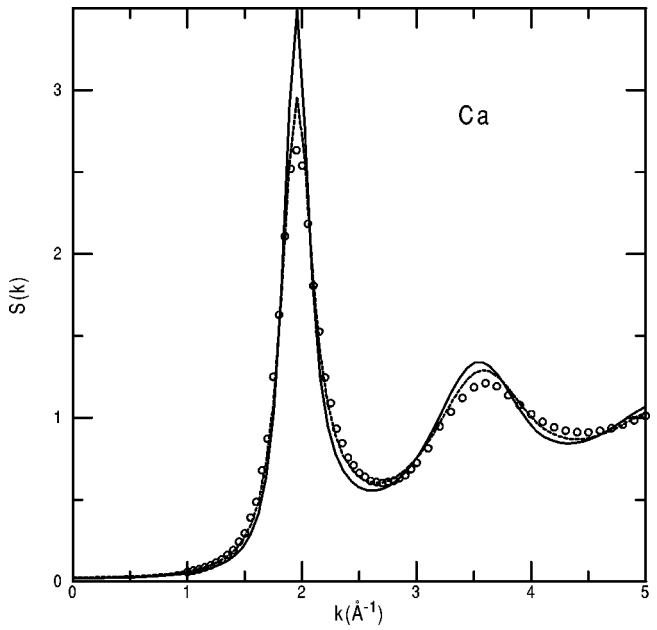

FIG. 10. $S(k)$ of liquid Ca at $T=1123$ K and $\rho=0.02058A^{-3}$. Notations are the same as in Fig. 2.

due to the approximation introduced in the PHNC, but due to the possible inaccuracy of the pair interactions derived from the OMP. As noted by Wax *et al.*, oscillations in the BG $g(r)$ are shifted toward smaller interionic distances compared to the experimental data for K and Rb, and this is the reason why we are particularly interested in these two metals other than Na and Cs. With the AH set, we find that this kind of shift is diminished, and the calculated results are in better agreements with experimental data. As was noted in Table II, this is also manifested in the better quality of thermodynamic values calculated with the AH set. Although we have not shown here, the PHNC calculations for the pair structures of Na and Cs give results similar to those observed by Wax *et al*. With the BG sets, the PHNC results, similar to the simulated data from the molecular dynamics calculations, agree well with experimental data.

Figure 5 shows the OMP $V(r)$ for alkaline-earth metals calculated from Eq. (2.4). Our results can be compared with Fig. 2 of Ref. 23 obtained from the NPA. For Be, we note that there is a large difference in the two results of $V(r)$. In the OMP, the position of the global minumum (r^*) of $V(r)$ is located at the position of the second minimum at $r\sim7.51$ a.u. On the other hand, it is observed at the first minimum around $r\sim4.0$ a.u. in the NPA. For other alkaline-earth metals, Friedel oscillations are much weaker, and we

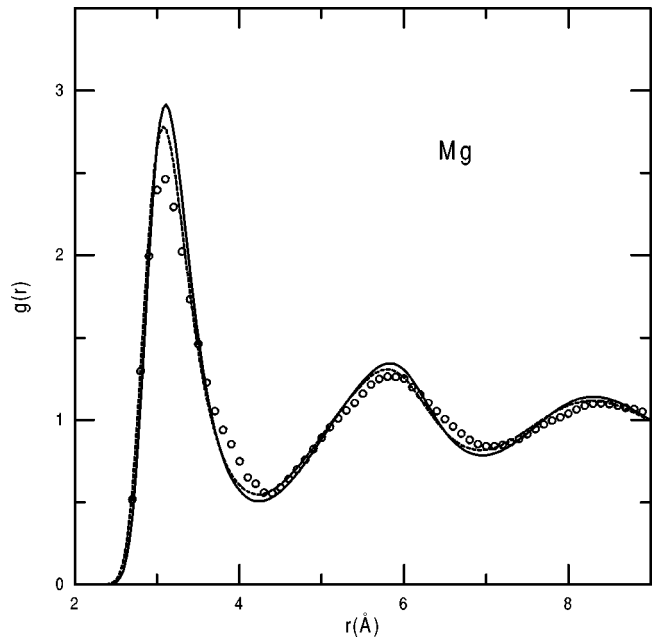

FIG. 9. $g(r)$ of liquid Mg at $T=953$ K and $\rho=0.03829A^{-3}$. Notations are the same as in Fig. 2.

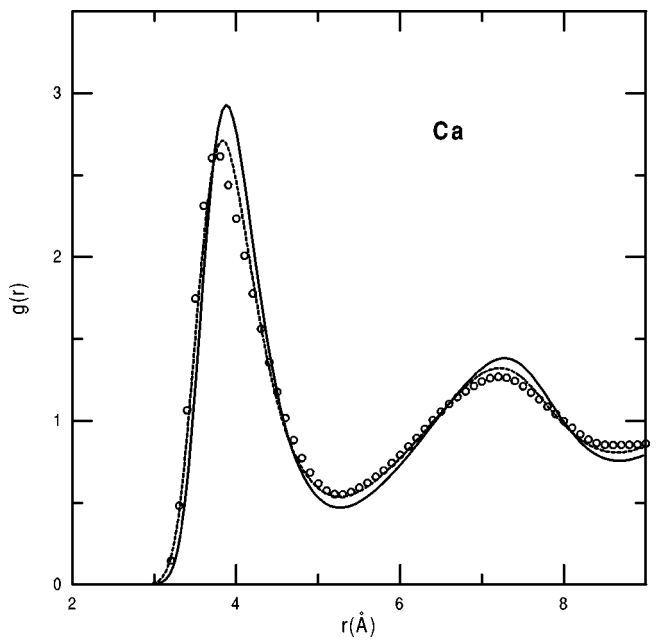

FIG. 11. $g(r)$ of liquid Ca at $T=1123$ K and $\rho=0.02058\ A^{-3}$. Notations are the same as in Fig. 2.

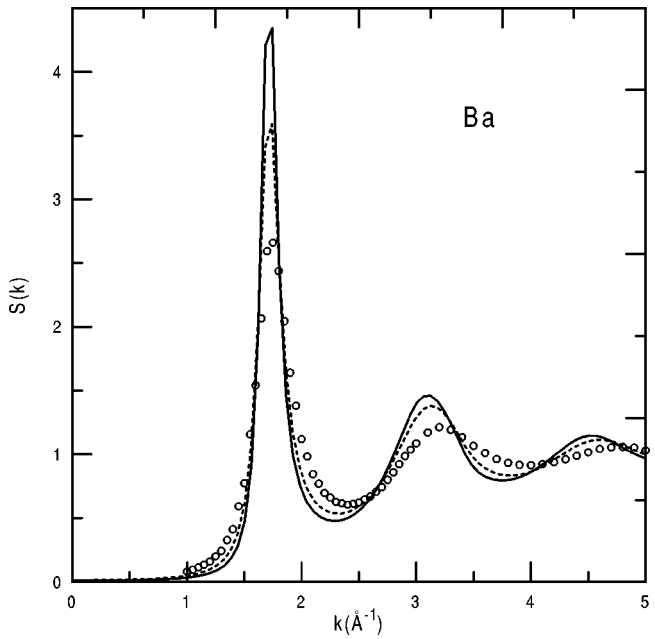

FIG. 12. $S(k)$ of liquid Ba at $T=1003$ K and $\rho=0.01456A^{-3}$. Notations are the same as in Fig. 2.

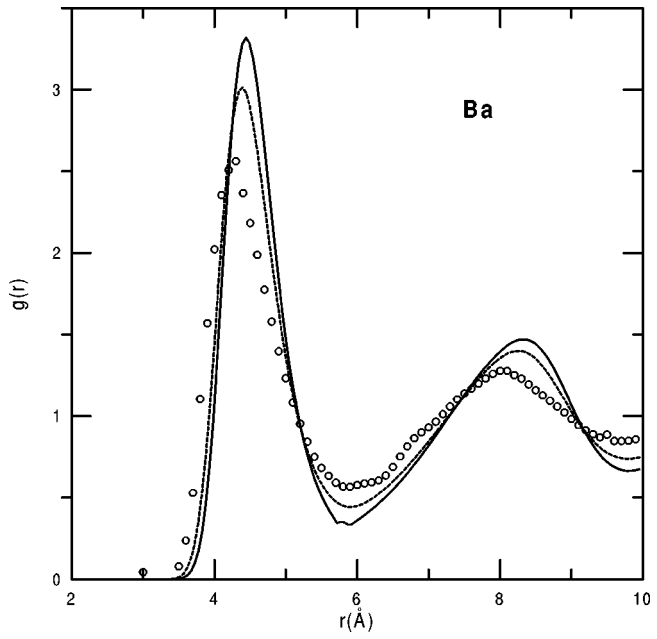

FIG. 13. $g(r)$ of liquid Ba at $T=1003$ K and $\rho=0.01456A^{-3}$. Notations are the same as in Fig. 2.

find that there is only one minimum of appreciable magnitude. Furthermore, the positions of r^* are approximately the same in the two methods except for Ba. For example, it is located at $r\sim 6$ a.u. for Mg. However, the well depth of potential minimum is much shallower in the OMP. For Ca, $V(r^*)\sim -0.64$ and -0.47 kT for the OMP with the AH and the BG parameters, respectively. For the NPA, the corresponding value is aprroximately -1.81 kT. Reference to Fig. 3 of Ref. 23 shows that the depth observed for the OMP is even shallower than those from Harrison's optimized pseudopotential obtained by Jank and Hafner.[39] In our figure, vertical dashed lines show the repulsive range λ of each metal calculated from Eq. (2.9). They are equal to r^* for Mg and Ca.0 This is the same for all the alkali metals described above. One the other hand, Be and Ba have λ values on the repulsive side of the first minimum.

Figures 6–13 show $S(k)$ and $g(r)$ for liquid beryllium, magnesium, calcium, and barium at thermodynamic states considered in Table II. With the BG set of the OMP parameters, not with the AH, the PHNC calculations give good results at the successive maxima in $S(k)$ and $g(r)$ for Mg and Ca. For Be, there is no experimental data available. Comparisons of our results with the NPA results given in Figs. 4 and 5 of Ref. 23 show that the PHNC exhibits quality similar to the NPA. In fact, the NPA implies NPA +VMHNC, which means that the pair structures were calculated from the VMHNC, using the pair interactions derived from the NPA. For Be, it is surprising that our result agrees well with the NPA data, noting that there is a large difference in two $V(r)$, as was described in the previous paragraph. Furthermore, this shows that the PHNC does not require any specific treatment when there is more than one potential minimum at $r<r^*$. We need a further investigation to clarify if this is generally the case. Agreements with experimental data are poor for thermodynamics and the pair structures of Ba calculated from the present method. This observation is closely related to the finding that, unlike other alkaline-earth metals, nearly a half of the valence electrons for Ba exhibits the *d*-character at the normal density.[39–41] Related to this problem, Moriarty pointed out that the proper value of the valence charge Z_+ of Ba is 1.25,[40] not 2 (as we have assumed). Therefore, Ba lies outside the scope of the pseudo-

TABLE V. Comparison of thermodynamic properties of liquid lithium calculated from the present work (OMP) with experimental data (Ref. 42) and neutral pseudoatom method (NPA) (Ref. 22). Two sets of data are shown for the OMP. The first line corresponds to the AH set of the OMP parameters, and the second, for the BG set.

		E_{bind}/kT			$P/\rho kT$			S^e/k		
T (K)	$\rho(A^{-3})$	Exp	OMP	NPA	Exp	OMP	NPA	Exp	OMP	NPA
470	0.044512	−176.91	−171.14	−184.35	0.0	3.49	2.80	−3.37	−3.93	−3.37
			−171.31			−2.23			−3.77	
595	0.043	−138.75	−135.05	−144.60	0.0	1.48	1.30	−2.90	−3.39	−2.88
			−137.33			−2.48			−3.23	
725	0.042	−113.87	−110.21	−117.97	0.0	1.15	−2.25	−2.52	−3.00	−2.50
			−112.03			−1.90			−2.86	

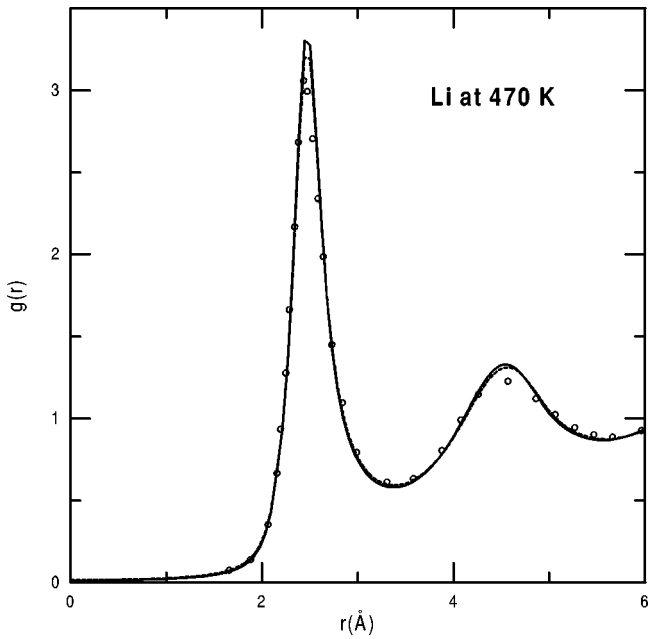

FIG. 14. $g(r)$ of liquid Li at $T=470$ K and $\rho=0.044512A^{-3}$. Open circles represent experimental data due to Olbrich *et al.* (Ref. 43). Other notations are the same as in Fig. 2.

potential theory for the s,p-bonded metals. In short, with the BG set of the OMP parameters, the pair structures from the OMP+PHNC are reliable for Be, Mg, and Ca.

We finally consider liquid lithium. Since this metal does not have a p electron in the core, the p component of valence electrons cannot be pseudized. This implies a strong electron-ion potential, and it can invalidate the idea of the weak pseudopotential. Table V compares $E_{\text{bind}}, Z=P/\rho kT$, and S^e/k for liquid lithium calculated from the OMP+PHNC with experimental data and recent calculations based on the NPA+VMHNC due to Gonzalez *et al.*[23] Compared with the NPA results, the table shows that the quality of our values of E_{bind} are better with either of the AH or the BG parameters. Unlike other alkali metals, the BG set gives slightly better results than the AH for E_{bind}. On the other hand, our results on S^e are less reliable than the NPA+VMHNC. In Fig. 14 the PHNC $g(r)$ is also compared with experimental data at one of three states considered in Table V. Our theoretical curve is in excellent agreement with experimental data for both of the AH and the BG sets of the OMP parameters. Only a minor difference is observed between the two sets of theoretical results, in that the AH predicts that the first peak is slightly higher. Similar behaviors were observed at other two states considered in Table V. This is also true for the state considered by Wax *et al.* in their Fig. 5.[13]

IV. DISCUSSION

We have shown that the combination of the OMP and the PHNC can be successfully applied to the study of liquid alkali and the first three alkaline-earth metals. Although a careful choice was necessary for the method in which the OMP parameters are calculated, the quality of our results are comparable to those from one of the most reliable *ab initio* methods for calculating the pair structures and the thermodynamic properties of simple metals, i.e., from the combination of the NPA and the VMHNC. The present calculations are based on a simple method for choosing the respulsive range of the pair potential, as given in Eq. (2.9). This would not be the only method for choosing λ. As in the VMHNC, it can be chosen to minimize the Helmholtz free energy, a problem which needs further investigation. At present, we are more interested in applying the present method for the study of pair structures in the expanded and compressed liquid metals, and its results will be reported later.

ACKNOWLEDGMENTS

The completion of this work was possible by the support from the Agency for Defense Developement of Korea, Korea Research Foundation, and Jeonju University.

[1] W.A. Harrison, in *Pseudopotentials in the Theory of Metals* (Benjamin, New York, 1966).
[2] N.E. Cusak, in *The Physics of Structurally Disordered Matter* (Adam Hilgher, Bristol, 1987).
[3] M. Hasegawa, K. Hoshino, M. Watabe, and W.H. Young, J. Non-Cryst. Solids **117/118**, 300 (1990).
[4] D.J. Gonzalez, D.A. Ng, and M. Silbert, J. Non-Cryst. Solids **117/118**, 469 (1990).
[5] N. Matsuda, H. Mori, K. Hoshino, and M. Watabe, J. Phys.: Condens. Matter **3**, 827 (1991).
[6] R.W. Shaw, Phys. Rev. **174**, 769 (1968).
[7] R.W. Shaw, J. Phys. C **2**, 2335 (1969).
[8] R.W. Shaw, J. Phys. C **3**, 1140 (1970).
[9] J.L. Bretonnet and C. Regnaut, Phys. Rev. B **31**, 5071 (1985).
[10] C. Regnaut and J.L. Bretonnet, Phys. Rev. B **38**, 10 922 (1988).
[11] M. Boulahbak, J.-F. Wax, and J.L. Bretonnet, J. Phys.: Condens. Matter **9**, 4017 (1997).
[12] R. Kumaravadivel and R. Evans, J. Phys. C **9**, 3877 (1976).
[13] J.-F. Wax, N. Jakse, and J.-L. Bretonnet, Phys. Rev. B **55**, 12 099 (1997).
[14] H.S. Kang and F.H. Ree, J. Chem. Phys. **103**, 3629 (1995).
[15] H.S. Kang and F.H. Ree, J. Chem. Phys. **103**, 9370 (1995).
[16] H.S. Kang and F H. Ree, Phys. Rev. E **57**, 5988 (1998).
[17] F. Lado, S.M. Foiles, and N.W. Ashcroft, Phys. Rev. A **28**, 2374 (1983).
[18] Y. Rosenfeld, J. Stat. Phys. **42**, 437 (1986).
[19] G. Zerah and J.-P. Hansen, J. Chem. Phys. **84**, 2336 (1986).
[20] H.C. Chen and S.K. Lai, Phys. Rev. E **49**, R982 (1994).
[21] L.E. Gonzalez, D.J. Gonzalez, and M. Silbert, Physica B **168**, 39 (1991).
[22] L.E. Gonzalez, D.J. Gonzalez, M. Silbert, and J.A. Alonso, J. Phys.: Condens. Matter **5**, 4283 (1993).
[23] L.E. Gonzalez, A. Meyer, M.P. Iniguez, D.J. Gonzalez, and M. Silbert, Phys. Rev. E **47**, 4120 (1993).
[24] J.L. Bretonnet and N. Jakse, Phys. Rev. B **50**, 2880 (1994).
[25] M. Boulahbak, N. Jakse, J.-F. Wax, and J.-L. Bretonnet, J. Chem. Phys. **108**, 2111 (1998).
[26] E.G. Brovman and Y. Kagan, Zh. Éksp. Theor. Fiz. **57**, 1329 (1969) [Sov. Phys. JETP **30**, 721 (1970)].
[27] A.O.E. Animalu and V. Heine, Philos. Mag. **12**, 1249 (1965).
[28] E.R. Cowley, Can. J. Phys. **54**, 2348 (1976).
[29] L.E. Ballentine and O.P. Gupta, Can. J. Phys. **49**, 1549 (1971).

[30] S. Ichimaru and K. Utsumi, Phys. Rev. B **24**, 7385 (1981).
[31] P. Ballone, G. Pastore, G. Galli, and D. Gazzillo, Mol. Phys. **59**, 275 (1986).
[32] M.J. Gillan, Mol. Phys. **38**, 1781 (1979).
[33] K. A. Schneider, in *Solid State Physics: Advances in Research and Applications*, edited by F. Seitz and D. Turnbull (Academic, New York, 1964), Vol. 16, p. 275.
[34] W.H. Young, Rep. Prog. Phys. **55**, 1769 (1992).
[35] A.B. Walker and R. Taylor, J. Phys.: Condens. Matter **2**, 9481 (1990).
[36] Y. Waseda, in *Condensed Matter: Disordered Solids*, edited by S. K. Srivastava and N. H. March (World Scientific, London, 1995), p17.
[37] Y. Waseda, in *The Structure of Non-Crystalline Materials* (McGraw-Hill, New York, 1980).
[38] W. van der Lugt and B. P. Alblas, in *Handbook of Thermodynamic and Transport Properties of Alkali Metals*, edited by R. W. Ohse (Blackwell, Oxford, 1985), Chap. 5.1.
[39] W. Jank and J. Hafner, Phys. Rev. B **42**, 6926 (1990).
[40] J.A. Moriarty, Phys. Rev. B **28**, 4818 (1983); **34**, 6738 (1986).
[41] H.L. Skriver, Phys. Rev. B **31**, 1909 (1985).
[42] *Handbook of Thermodynamic and Transport Properties of Alkali Metals*, edited by R. W. Ohse (Blackwell, Oxford, 1985).
[43] H. Olbrich, H. Ruppersberg, and S. Steeb, Z. Naturforsch. A **38**, 1328 (1983).